Jian-Jun Fan, Yaoling Niu, Yi-Ming Liu, and Yu-Jie Hao, 2020, Timing of closure of the Meso-Tethys Ocean: Constraints from remnants of a 141–135 Ma ocean island within the Bangong–Nujiang Suture Zone, Tibetan Plateau: GSA Bulletin, https://doi.org/10.1130/B35896.1.

Supplemental Material

Text S1. Analytical methods

Figure S1. Zircon U-Pb and whole-rock Ar-Ar ages from the basalt and gabbro in the Zhonggang igneous–sedimentary rocks reported by previous studies

Figure S2. Plots of immobile elements vs. MgO for the Zhonggang basalt and trachyandesite

Table S1. Whole-rock major (wt%) and trace element (ppm) data of the basalt and trachyandesite in the Zhonggang igneous–sedimentary rocks

Table S2. Zircon LA–ICP–MS U–Pb data of the trachyandesite in the Zhonggang igneous–sedimentary rocks

Table S3. Whole-rock Sr–Nd isotopic composition of the basalt and trachyandesite in the Zhonggang igneous–sedimentary rocks

TEXT S1. ANALYTICAL METHODS

1. Whole-rock major and trace element analyses

Samples were trimmed to remove weathered surfaces, cleaned with deionized water, crushed, and powdered in an agate mill. Major element compositions were analyzed by inductively coupled plasma-optical emission spectroscopy (ICP-OES; Leeman Prodigy) with high-dispersion Echelle optics at the Key Laboratory of Mineral Resources Evaluation in Northeast Asia, Ministry of Natural Resources of China, Changchun, China. Loss on ignition (LOI) values were determined by heating 1 g of sample in a furnace at 1000 °C for several hours before being cooled in a desiccator and reweighed. Analytical uncertainties for the major elements are <1 wt%. Trace element compositions were analyzed by inductively coupled plasma-mass spectrometry (ICP-MS; Agilent-7900). The analytical accuracy and precision during trace element analysis were determined from standards AGV-2 (U.S. Geological Survey standard) and GSR-3 (Chinese national geological reference standard). The analytical accuracy is <5 wt% for most elements. The values obtained for the standards are in good agreement with recommended values (Govindaraju, 1994).

2. Zircon U-Pb dating

Zircon grains were separated by crushing, conventional heavy liquid and magnetic techniques from sandstone samples in the Laboratory of the Geological Team of Hebei Province, Langfang, China. The internal structures of zircon were characterized using cathodoluminescence (CL) in the Continental Dynamics Laboratory, Chinese Academy of Geological Sciences, Beijing, China to select spots for laser ablation-inductively coupled plasma-mass spectroscopy (LA-ICP-MS) analysis. LA-ICP-MS U-Pb zircon dating was carried out in the Key Laboratory of Mineral Resources Evaluation in Northeast Asia, Ministry of Natural Resources of China, Changchun, China. The spot size was 24 μm for each sample. Helium was used as a carrier gas. Reference and internal zircon standards 91500 (Wiedenbeck et al., 1995) and NIST610 (^{29}Si), respectively, were used for instrumental calibration. The Pb correction method of ~~Anderson~~ Andersen (2002) was applied with analytical details following Yuan et al. (2004). Reported uncertainties for the age analyses are given as 1σ values with weighted mean ages in the 95% confidence level. Isotopic data were processed using the GLITTER (version 4.4) and Isoplot/Ex (version 3.0) programs (Ludwig, 2003). The ages reported are ^{206}Pb/^{238}U ages for grains<1000 Ma and ^{207}Pb/^{206}Pb ages for grains >1000 Ma. For statistical purpose, zircon ages with a discordance of <10% was considered to be usable.

3. Whole-rock Sr-Nd isotopes

Whole-rock Sr-Nd isotopic analyses were undertaken by Nanjing FocuMS Technology. Prior to analysis, sample powders were dissolved in a mixture of HF, HNO_3, and $HClO_4$ in Teflon bombs and separated by routine cation-exchange techniques. Sr-Nd isotopic measurements were performed using a Nu Plasma II MC-ICP-MS. Mass fractionation corrections and adjustments for instrumental drift for Sr isotopic ratios were based on ^{86}Sr/^{88}Sr = 0.1194, and the analyzed composition of the NIST SRM 987 isotopic standard, respectively. Mass fractionation and instrumental drift corrections for Nd isotopic ratios were based on $^{146}Nd/^{144}Nd = 0.7219$, and the analyzed composition of the JNdi-1 isotopic standard, respectively.

REFERENCES CITED

Andersen, T., 2002, Correction of common lead in U-Pb analyses that do not report ^{204}Pb: Chemical Geology, v. 192, p. 59–79, https://doi.org/10.1016/S0009-2541(02)00195-X.

Govindaraju, K., 1994, Compilation of working values and sample description for 383 geostandards: Geostandards Newsletter, v. 18, p. 1–158, https://doi.org/10.1111/j.1751-908X.1994.tb00502.x.

Ludwig, K.J., 2003, ISOPLOT 3.0: Berkeley Geochronology Center Special Publication, v. 4, p. 70.

Wiedenbeck, M., Allé, P., Corfu, F., Griffin, W.L., Meier, M., Oberli, F., Quadt, A.V., Roddick, J.C., and Spiegel, W., 1995, Three natural zircon standards for U-Th-Pb, Lu-Hf,trace element and REE analyses: Geostandards and Geoanalytical Research, v. 19, p. 1–23, https://doi.org/10.1111/j.1751-908X.1995.tb00147.x.

Yuan, H.L., Gao, S., Liu, X.M., Li, H.M., Günther, D., and Wu, F.Y., 2004, Accurate U-Pb age and trace element determinations of zircon by laser ablation-inductively coupled plasma mass spectrometry: Geostandards and Geoanalytical Research, v. 28, p. 353–370, https://doi.org/10.1111/j.1751-908X.2004.tb00755.x.

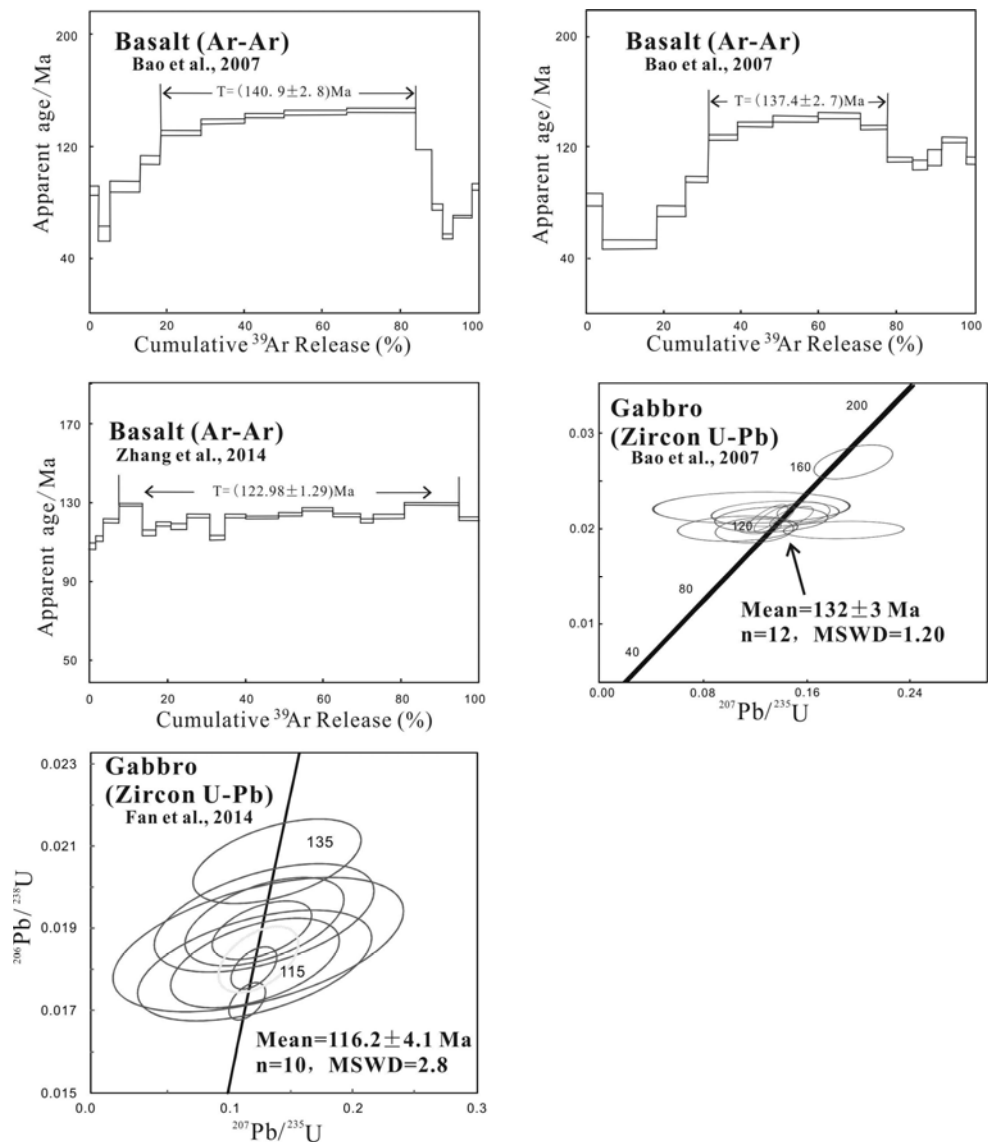

Figure S1. Zircon U-Pb and whole-rock Ar-Ar ages from the basalt and gabbro in the Zhonggang igneous-sedimentary rocks reported by previous studies

REFERENCES CITED

Bao, P.S., Xiao, X.C., Su, L., and Wang, J., 2007, Petrological, geochemical and chronological constraints for the tectonic setting of the Dongco ophiolite in Tibet: Science China. Earth Sciences, v. 50, p. 660–671, https://doi.org/10.1007/s11430-007-0045-5.

Fan, J.J., Li, C., Xie, C.M., and Wang, M., 2014, Petrology, geochemistry, and geochronology of the Zhonggang ocean island, northern Tiber: implications for the evolution of the Bangongco-Nujiang oceanic arm of Neo-Tethys: International Geology Review, v. 56, p. 1504–1520, https://doi.org/10.1080/00206814.2014.947639.

Zhang, K.J., Xia, B., Zhang, Y.X., Liu, W.L., Zeng, L., Li, J.F., and Xu, L.F., 2014, Central Tibetan Meso-Tethyan oceanic plateau: Lithos, v. 210–211, p. 278–288, https://doi.org/10.1016/j.lithos.2014.09.004.

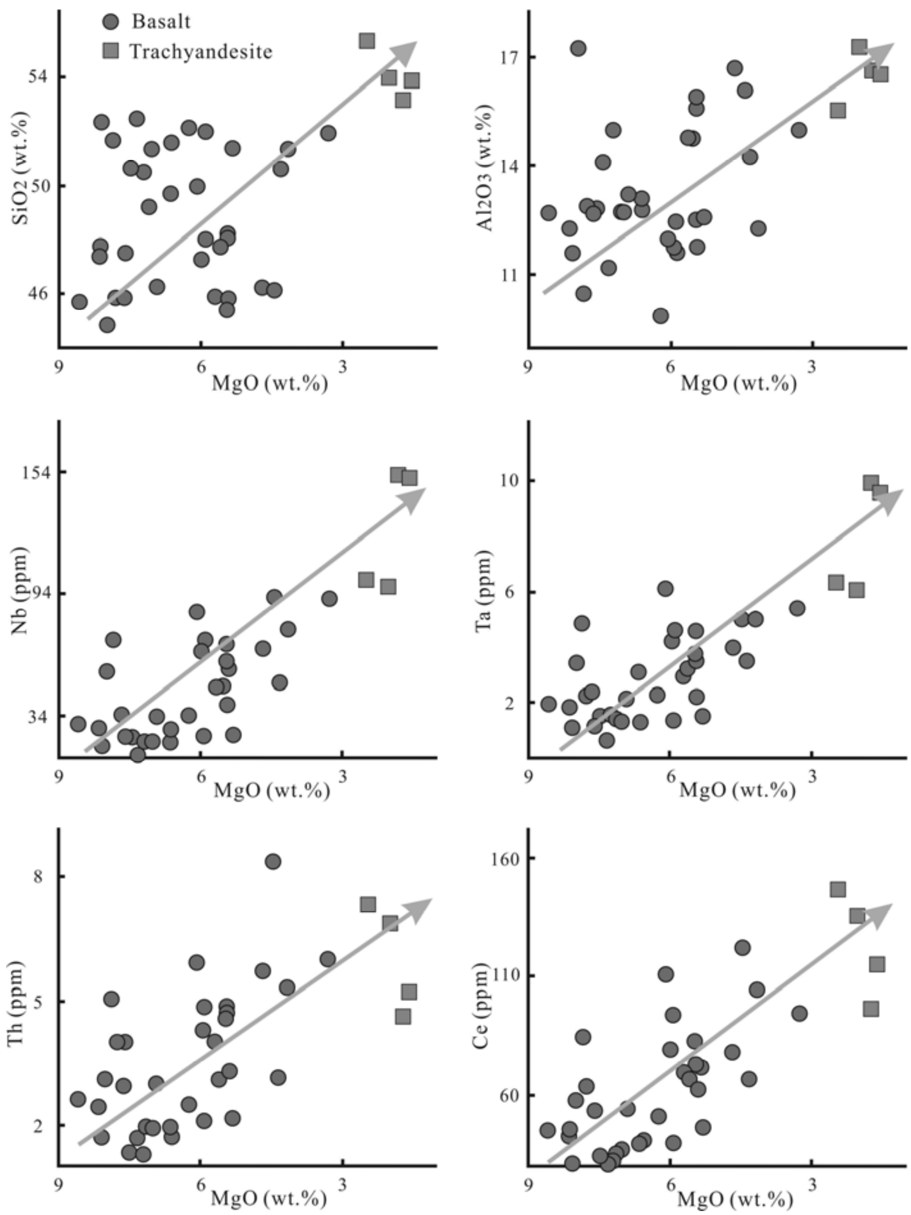

Figure S2. Plots of immobile elements versus MgO for the Zhonggang basalt and trachyandesite

Table S1. Whole-rock major (wt%) and trace element (ppm) data of the basalt and trachyandesite in the Zhonggang igneous-sedimentary rocks

Sample	B19T84H1	B19T84H2	Oz3H1	Oz3H2	Oz3H3	Oz3H4	Oz3H5	Oz3H6	Oz3H7	Oz2H3	Oz2H2	Oz2H1	Oz4H3	Oz4H2	Oz4H1
Reference	This study		Fan et al., 2014												
Lithology	basalt	basalt	basalt	basalt	basalt	basalt	basalt	basalt	basalt	basalt	basalt	basalt	basalt	basalt	basalt
SiO_2	45.8	45.8	51.4	49.2	52.3	51.6	52.0	48.1	51.3	44.9	50.6	50.5	49.7	47.7	50.6
TiO_2	2.88	2.85	3.04	2.66	2.27	2.35	2.67	4.24	2.67	2.67	2.19	1.90	2.11	3.89	3.60
Al_2O_3	12.9	12.7	12.6	12.7	11.6	12.9	12.5	11.8	12.7	17.2	14.1	15.0	13.1	14.8	14.3
Fe_2O_3T	12.4	12.3	12.1	12.3	10.3	11.3	11.7	16.3	11.5	13.5	9.65	8.73	10.9	12.7	11.0
MnO	0.17	0.16	0.13	0.14	0.13	0.14	0.13	0.20	0.14	0.24	0.12	0.11	0.13	0.16	0.14
MgO	7.72	7.65	5.30	7.07	8.07	6.61	5.9	5.41	7.0	7.98	7.45	7.21	6.62	5.59	4.35
CaO	10.9	11.31	6.87	7.95	7.73	6.75	6.73	5.7	6.48	3.95	8.81	9.16	9.41	7.42	7.27
Na_2O	2.66	2.84	4.44	4.43	3.65	4.36	4.3	3.51	4.1	3.87	2.91	3.26	2.89	2.93	3.43
K_2O	1.18	0.91	1.41	1.19	1.29	1.3	1.36	2.2	1.51	0.27	0.73	0.57	0.94	1.38	2.35
P_2O_5	0.37	0.4	0.35	0.29	0.27	0.29	0.31	0.51	0.28	0.43	0.21	0.19	0.25	0.34	0.36
LOI	2.99	2.97	1.40	1.39	1.27	1.09	0.97	1.13	1.04	3.94	2.45	2.51	3.27	2.23	1.67
Cr	303	361	129	298	208	239	196	19.2	240	359	309	344	336	73.3	52.6
Ni	107	123	72.6	118.4	72.4	97.4	83.1	52.3	94.9	161	137	168	176	55.4	43.2
Rb	59.2	33.4	15.9	12.8	14.5	15.6	16	24.5	21	9.37	13.4	9.69	17.8	22.2	34.1
Sr	165	168	304	474	234	303	230	435	427	335	339	255	759	480	172
Y	32.4	32.4	26.4	22.8	20.8	23.3	23.9	36.4	23.2	27.4	25.4	23.3	25.0	29.0	28.7
Zr	249	250	185	160	148	152	170	275	150	219	165	150	169	283	275
Nb	34.0	34.2	25.4	21.8	19.5	21.8	23.7	39.3	22.1	56.2	23.3	20.8	27.7	49.4	50.6
Cs	1.28	1.06	0.02	0.02	0.04	0.02	0.02	0.02	0.04	2.09	0.18	0.13	0.11	0.16	0.24
Ba	313	317	136	116	147	144	145	196	274	155	270	140	238	565	404
La	29.2	30.0	21.2	15.4	12.3	18.3	17	26.9	16.2	26.7	14.4	13.8	17.4	29.7	30.1
Ce	64.9	66.7	46.2	35.3	30.2	40	39.9	62.5	36.9	58.0	34.5	32.6	39.4	65.9	66.8
Pr	7.92	8.08	5.96	4.69	4.15	5.21	5.27	8.25	4.86	7.60	4.86	4.59	5.34	8.77	8.77
Nd	36.0	36.7	26.4	21.1	19	23.1	23.5	36.7	21.8	32.1	22.2	21.0	23.6	38.0	37.9
Sm	8.37	8.47	6.19	5.13	4.7	5.47	5.5	8.63	5.24	7.07	5.60	5.27	5.64	8.58	8.48
Eu	2.65	2.61	2.05	1.74	1.48	1.86	1.79	2.57	1.78	2.31	1.74	1.76	1.95	2.92	2.72
Gd	7.92	8.03	6.3	5.24	4.81	5.59	5.6	8.66	5.4	6.78	5.84	5.50	5.82	8.30	8.07
Tb	1.16	1.17	0.94	0.8	0.73	0.83	0.84	1.29	0.81	0.96	0.87	0.82	0.85	1.15	1.11
Dy	6.81	6.93	5.33	4.59	4.17	4.73	4.83	7.36	4.64	5.51	5.11	4.79	4.98	6.28	6.11
Ho	1.26	1.27	0.99	0.85	0.77	0.87	0.9	1.36	0.86	1.02	0.94	0.88	0.93	1.10	1.07
Er	3.23	3.24	2.61	2.26	2.04	2.31	2.38	3.63	2.27	2.78	2.55	2.38	2.53	2.80	2.75
Tm	0.42	0.43	0.34	0.3	0.27	0.3	0.31	0.48	0.3	0.36	0.32	0.31	0.32	0.35	0.33
Yb	2.49	2.52	2.08	1.79	1.61	1.83	1.91	2.93	1.81	2.25	1.99	1.89	1.99	2.07	2.01
Lu	0.36	0.36	0.29	0.25	0.22	0.25	0.27	0.41	0.25	0.31	0.28	0.26	0.28	0.28	0.27
Hf	6.40	6.46	4.47	3.83	3.55	3.9	4.16	6.8	3.87	5.10	4.09	3.86	4.18	6.53	6.37
Ta	2.27	2.31	1.5	1.28	1.13	1.27	1.36	2.23	1.28	3.44	1.50	1.44	3.09	3.19	3.49
Pb	1.83	1.87	1.52	1.31	1.03	1.25	1.24	4.35	4.83	2.23	0.80	0.71	1.37	1.80	1.82
Th	3.99	4.01	2.13	1.95	1.72	1.95	2.06	3.29	1.92	3.10	1.36	1.32	1.75	3.06	3.18
U	1.03	1.04	0.48	0.42	0.37	0.42	0.44	0.74	0.43	0.81	0.43	0.39	0.36	0.95	0.90

Continued Table S1

Sample	DC13T1H3	DC13T1H4	DC13T1H5	DC13T1H6	DC13T1H7	DC13T1H10	DC13T1H11	DC13T1H14	11DC-23	11DC-25	11DC-26	11DC-27	11DC-28	11DC-30	11DC-40	11DC-41	11DC-42	11DC-43	11DC-44	D18T22H1	D18T22H2	DC13T1H8	DC13T1H9
Reference	Yu et al., 2016								Wang et al., 2016											This study		Yu et al., 2015	
Lithology	basalt	basalt	basalt	basalt	basalt	basalt	basalt	basalt	basalt	basalt	basalt	basalt	basalt	basalt	basalt	basalt	basalt	basalt	basalt	Trachyandesite	Trachyandesite	Trachyandesite	Trachyandesite
SiO_2	47.3	50.0	51.7	51.3	48.2	52.1	48.0	51.9	47.5	45.8	45.4	46.2	46.1	45.9	52.5	45.7	47.5	46.2	47.7	53.2	53.8	54.0	55.4
TiO_2	4.57	4.02	3.57	4.35	4.56	2.67	4.30	2.12	3.06	3.31	3.42	3.55	3.40	3.63	2.38	3.25	3.02	3.58	2.98	1.78	1.82	2.00	2.21
Al_2O_3	11.8	12.0	10.5	12.3	12.5	9.9	11.7	15.0	12.8	15.9	15.7	16.7	16.1	14.8	11.2	12.7	12.3	13.2	12.3	16.6	16.5	17.3	15.5
Fe_2O_3T	13.2	11.6	11.4	12.3	13.1	9.75	14.0	10.0	13.1	12.8	13.1	12.7	12.9	12.3	10.2	13.1	12.2	12.9	11.9	10.6	10.7	6.78	8.82
MnO	0.17	0.13	0.12	0.15	0.17	0.12	0.19	0.13	0.16	0.18	0.20	0.21	0.21	0.15	0.12	0.16	0.18	0.18	0.16	0.12	0.10	0.13	0.12
MgO	5.95	6.07	7.85	4.16	5.45	6.23	5.90	3.29	7.58	5.42	5.44	4.66	4.44	5.67	7.32	8.56	8.12	6.91	8.12	1.73	1.58	2.01	2.46
CaO	9.17	7.04	6.83	8.60	8.00	10.58	8.63	8.34	7.60	6.67	7.90	6.89	5.98	8.76	8.88	8.28	8.87	7.97	8.76	3.61	3.64	7.01	5.74
Na_2O	2.04	2.02	3.92	2.54	1.77	2.27	2.17	3.97	3.81	3.70	4.07	4.69	4.28	4.40	3.95	2.51	3.29	1.58	3.72	8.21	8.37	6.06	5.26
K_2O	1.71	4.44	0.93	1.51	2.92	2.30	2.60	0.55	0.50	1.58	0.38	1.15	2.60	0.13	1.64	1.84	1.27	4.02	1.01	0.52	0.47	0.76	1.39
P_2O_5	0.47	0.63	0.50	0.57	0.47	0.26	0.52	0.76	0.29	0.41	0.39	0.37	0.84	0.33	0.15	0.21	0.26	0.32	0.24	1.23	1.24	0.65	0.71
LOl	3.23	1.89	2.05	1.61	2.49	3.36	1.61	3.18	3.54	3.47	3.82	2.77	3.12	3.76	1.59	3.50	2.98	3.08	3.04	2.23	1.81	2.56	1.67
Cr	37.1	85.8	130	15.1	20.7	487	36.3	2.22	100	36	38	31	23	40	297	272	327	114	232	11.5	4.56	58.3	20.3
Ni	46.5	62.0	86.0	34.8	42.9	219	63.7	4.34	54.4	31.2	33.4	10.4	15.2	38.5	147	139	148	70.9	121	80.6	74.9	18.4	15.0
Rb	38.3	113	20.1	29.8	67.8	49.4	57.6	9.95	8.18	61.4	10.2	29.4	57.6	1.3	44.5	23.1	15.6	39.4	14.2	2.88	1.50	15.0	37.0
Sr	1279	79.3	91.1	1036	608	397	392	271	191	355	403	571	417	221	81.5	181	155	258	154	285	299	705	490
Y	33.0	40.0	32.1	42.2	34.3	24.5	36.4	25.5	29.4	30.8	31.1	30.9	36.6	32.0	24.1	28.3	27.6	31.9	26.5	45.5	50.2	38.3	43.3
Zr	290	391	300	408	299	197	331	244	226	330	336	299	408	312	161	221	209	244	201	1056	1060	417	478
Nb	66.4	85.6	71.3	76.3	68.7	34.4	70.4	91.0	23.9	58.9	60.1	66.9	91.6	48.1	14.7	30.5	28.6	34.2	28.0	151	151	98	101
Cs	0.72	1.06	0.35	0.45	1.09	0.57	0.67	0.75	0.69	0.68	0.50	2.16	2.92	0.23	0.42	0.35	0.33	0.26	0.32	0.13	0.10	3.85	0.74
Ba	146	326	68	266	305	442	282	132	295	396	324	824	778	133	72.0	392	344	852	294	54.0	51.7	501	322
La	35.0	45.5	38.3	42.3	36.8	21.7	39.7	45.0	23.4	34.3	34.4	37.2	59.3	30.7	12.3	19.2	19.8	24.0	18.9	38.4	47.0	57.3	59.7
Ce	79.0	110	84.6	104	82.7	50.7	93.7	93.9	53.4	71.8	72.6	77.9	122	68.6	30.4	45.1	45.6	54.3	43.9	96.9	115	135	147
Pr	10.0	12.9	10.5	12.6	10.5	6.59	11.5	10.7	7.66	9.54	9.70	10.2	15.7	9.60	4.53	6.59	6.60	7.77	6.39	15.3	18.5	15.3	16.9
Nd	45.2	57.7	46.4	57.7	47.2	30.0	51.7	44.4	33.4	39.2	39.7	41.4	62.4	41.2	20.8	29.7	29.7	34.5	28.2	65.9	78.8	65.4	73.5
Sm	10.1	12.4	10.1	13.1	10.6	6.90	11.3	8.99	7.55	8.04	8.03	8.43	11.6	8.69	4.98	6.99	6.85	7.98	6.75	15.8	18.0	13.0	15.1
Eu	3.23	3.89	3.15	4.18	3.41	2.27	3.58	2.90	2.38	2.59	2.59	2.59	3.52	2.68	1.63	2.21	2.26	2.57	2.14	5.01	5.71	4.89	5.04
Gd	9.82	11.7	9.62	12.6	10.3	6.814	10.8	8.18	7.63	7.73	7.71	8.04	10.2	8.33	5.20	7.04	6.97	7.99	6.77	14.6	16.3	11.7	13.7
Tb	1.34	1.59	1.29	1.71	1.39	0.96	1.47	1.07	1.11	1.13	1.14	1.15	1.45	1.21	0.83	1.06	1.05	1.19	1.00	2.26	2.43	1.55	1.81
Dy	7.46	8.92	7.26	9.52	7.78	5.40	8.16	5.80	6.15	6.06	6.25	6.37	7.64	6.55	4.74	5.81	5.82	6.61	5.60	12.0	12.8	8.48	9.89

Ho	1.30	1.58	1.26	1.66	1.36	0.96	1.42	0.98	1.18	1.16	1.19	1.25	1.43	1.26	0.93	1.13	1.13	1.28	1.10	2.32	2.40	1.49	1.69
Er	3.43	4.22	3.35	4.32	3.58	2.54	3.75	2.49	2.92	2.95	3.09	3.05	3.57	3.09	2.32	2.75	2.75	3.05	2.69	6.11	6.34	3.95	4.45
Tm	0.42	0.53	0.42	0.54	0.44	0.32	0.46	0.30	0.39	0.42	0.41	0.41	0.48	0.41	0.32	0.36	0.37	0.40	0.34	0.87	0.87	0.50	0.55
Yb	2.55	3.24	2.53	3.28	2.68	1.96	2.79	1.78	2.26	2.58	2.64	2.60	2.93	2.48	1.87	2.22	2.14	2.37	2.13	4.91	5.03	3.01	3.39
Lu	0.34	0.43	0.33	0.43	0.36	0.26	0.36	0.23	0.34	0.38	0.40	0.38	0.42	0.36	0.27	0.31	0.30	0.36	0.30	0.77	0.76	0.41	0.45
Hf	7.31	9.47	7.28	10.16	7.61	5.08	8.29	4.53	5.46	7.13	7.38	6.58	8.61	7.02	3.89	5.35	5.13	5.82	4.96	22.6	23.5	9.16	11.0
Ta	4.32	6.08	4.76	5.02	4.58	2.28	4.58	5.45	1.20	3.65	3.76	3.91	5.01	2.99	0.62	1.94	1.83	2.10	1.79	9.93	9.60	6.03	6.34
Pb	2.65	2.33	2.20	3.21	2.80	1.82	2.04	1.94	1.67	2.55	4.26	4.27	6.64	1.87	1.90	1.39	1.19	1.84	2.10	4.63	4.29	1.63	2.64
Th	4.28	5.93	5.05	5.35	4.56	2.50	4.84	6.00	2.94	4.74	4.81	5.70	8.36	4.03	1.71	2.60	2.48	3.02	2.42	4.62	5.19	6.80	7.36
U	1.07	1.54	1.18	1.33	1.14	0.75	1.23	1.59	0.85	1.30	1.32	1.45	2.05	1.18	0.57	0.79	0.70	0.82	0.69	1.36	1.46	3.75	1.70

REFERENCES CITED

Fan, J.J., Li, C., Xie, C.M., and Wang, M., 2014, Petrology, geochemistry, and geochronology of the Zhonggang ocean island, northern Tiber: implications for the evolution of the Bangongco-Nujiang oceanic arm of Neo-Tethys: International Geology Review, v. 56, p. 1504–1520, https://doi.org/10.1080/00206814.2014.947639.

Wang, B.D., Wang, L.Q., Chung, S.L., Chen, J.L., Yin, F.G., Liu, H., Li, X.B., and Chen, L.X., 2016, Evolution of the Bangong-Nujiang Tethyan ocean: Insights from the geochronology and geochemistry of mafic rocks within ophiolites: Lithos, v. 245, p. 18–33, https://doi.org/10.1016/j.lithos.2015.07.016.

Yu, Y.P., Hu, P.Y., Li, C., Xie, C.M., Fan, J.J., Xu, W., and Liu, J.H., 2016, The Petrology and geochemistry of Early Cretaceous ocean island volcanic rocks in the middle-western segment of Bangong Co-Nujiang suture zone [in Chinese with English abstract]: Geological Bulletin of China, v. 35, p. 1281–1290.

Table S2. Zircon LA-ICP-MS U-Pb data of the trachyandesite in the Zhonggang igneous-sedimentary rocks

Spots	**isotope ratio（±1σ）**						**age（Ma±1σ）**					
	$^{207}Pb/^{206}Pb$		**$^{207}Pb/^{235}U$**		**$^{206}Pb/^{238}U$**		**$^{207}Pb/^{206}Pb$**		**$^{207}Pb/^{235}U$**		**$^{206}Pb/^{238}U$**	
	ratios	**1σ**	**ratios**	**1σ**	**ratios**	**1σ**	**age**	**ratio**	**age**	**1σ**	**age**	**1σ**
D18T21-1	0.04995	0.00135	0.1426	0.00432	0.02072	0.00051	193	32	135	4	132	3
D18T21-2	0.04929	0.0094	0.14986	0.0284	0.02207	0.00078	162	307	142	25	141	5
D18T21-3	0.04903	0.00428	0.14515	0.01236	0.02149	0.00074	149	128	138	11	137	5
D18T21-4	0.05046	0.00407	0.15789	0.01272	0.02271	0.00065	216	130	149	11	145	4
D18T21-5	0.04892	0.00398	0.14869	0.01183	0.02205	0.00072	144	119	141	10	141	5
D18T21-6	0.04887	0.00439	0.1529	0.01374	0.0227	0.00064	142	149	144	12	145	4
D18T21-7	0.05021	0.00186	0.15861	0.00608	0.02291	0.00055	205	47	149	5	146	3
D18T21-8	0.05104	0.00562	0.15552	0.01694	0.02215	0.00055	243	199	147	15	141	3
D18T21-9	0.05001	0.00819	0.15672	0.02545	0.02277	0.00065	195	284	148	22	145	4
D18T21-10	0.04695	0.01131	0.14121	0.03386	0.02185	0.00064	47	367	134	30	139	4
B19T63-1	0.04923	0.00399	0.15679	0.01255	0.02311	0.00059	159	133	148	11	147	4
B19T63-2	0.04805	0.00156	0.14525	0.00466	0.02191	0.00047	102	38	138	4	140	3
B19T63-3	0.04829	0.00213	0.14803	0.00636	0.02222	0.00051	114	59	140	6	142	3
B19T63-4	0.04913	0.00337	0.14539	0.00988	0.02145	0.00049	154	111	138	9	137	3
B19T63-5	0.05175	0.01159	0.1471	0.03262	0.02061	0.00079	274	361	139	29	132	5
B19T63-6	0.0491	0.00415	0.14964	0.01244	0.0221	0.00056	153	139	142	11	141	4
B19T63-7	0.05019	0.00257	0.14761	0.00741	0.02133	0.00047	204	76	140	7	136	3
B19T63-8	0.04937	0.00174	0.15926	0.00558	0.02339	0.00052	165	43	150	5	149	3
B19T63-9	0.04961	0.01211	0.14899	0.03608	0.02177	0.00082	177	377	141	32	139	5
B19T63-10	0.05042	0.01073	0.14448	0.0303	0.02077	0.00088	214	331	137	27	133	6
B19T63-11	0.05091	0.0084	0.14739	0.024	0.02099	0.00071	237	284	140	21	134	4
D18T22-1	0.04979	0.00213	0.14404	0.00645	0.02098	0.00054	185	58	137	6	134	3
D18T22-2	0.04929	0.00207	0.14401	0.00625	0.02119	0.00056	162	54	137	6	135	4
D18T22-3	0.04978	0.00244	0.15178	0.0076	0.02211	0.00059	185	68	143	7	141	4
D18T22-4	0.04887	0.00285	0.1428	0.00842	0.02119	0.00058	142	85	136	7	135	4
D18T22-5	0.05399	0.00244	0.16277	0.00759	0.02187	0.00057	371	59	153	7	139	4
D18T22-6	0.05134	0.00173	0.14525	0.00522	0.02052	0.00052	256	40	138	5	131	3
D18T22-7	0.04974	0.00189	0.14933	0.00596	0.02177	0.00056	183	48	141	5	139	4
D18T22-8	0.04834	0.00137	0.14021	0.00436	0.02103	0.00052	116	34	133	4	134	3

Table S3. Whole-rock Sr-Nd isotopic composition of the basalt and trachyandesite in the Zhonggang igneous-sedimentary rocks

Reference	Sample	Lithology	Rb	Sr	$^{87}Sr/^{86}Sr$	2σ	$^{87}Rb/^{86}Sr$	$(^{87}Sr/^{86}Sr)i$	Sm	Nd	$^{143}Nd/^{144}Nd$	2σ	$^{147}Sm/^{144}Nd$	$(^{143}Nd/^{144}Nd)i$	$\varepsilon_{Nd}(t)$
This study	D18T22	Trachyandesite	1.50	299	0.704043	0.000038	0.0145	0.704014	18.0	78.8	0.512813	0.000005	0.1377	0.512686	4.46
	Oz4H2	basalt	22.2	480	0.705694	0.000003	0.1336	0.705428	8.58	38.0	0.512781	0.000005	0.1359	0.512657	3.88
	Oz2H1	basalt	9.69	255	0.705568	0.000004	0.1098	0.705349	5.27	21.0	0.512796	0.000005	0.1511	0.512658	3.91
	DC13T1H3	basalt	38.3	1279	0.704459	0.000004	0.0865	0.704286	10.1	45.2	0.512804	0.000004	0.1347	0.512681	4.35
	DC13T1H9	Trachyandesite	37	490	0.704803	0.000003	0.2186	0.704367	15.1	73.5	0.512810	0.000005	0.1241	0.512697	4.66
	DC13T1H14	basalt	9.95	271	0.704472	0.000004	0.1063	0.704260	8.99	44.4	0.512828	0.000005	0.1219	0.512716	5.04
Wang et al., 2016	11 DC-25	basalt	61.4	355	0.705266	0.000004	0.5003	0.704270	8.04	39.2	0.512825	0.000005	0.1236	0.512712	4.96
	11 DC-26	basalt	10.2	403	0.704246	0.000005	0.0732	0.704100	8.03	39.7	0.512831	0.000006	0.1218	0.512719	5.10
	11 DC-27	basalt	29.4	571	0.704604	0.000004	0.1489	0.704308	8.43	41.4	0.512805	0.000005	0.1227	0.512693	4.58
	11 DC-28	basalt	57.6	417	0.705626	0.000004	0.3996	0.704831	11.6	62.4	0.512830	0.000006	0.1120	0.512727	5.26
	11 DC-30	basalt	1.26	221	0.704025	0.000005	0.0165	0.703992	8.69	41.2	0.512875	0.000007	0.1271	0.512759	5.87
	11 DC-40	basalt	44.5	81.5	0.707281	0.000004	1.5798	0.704137	4.98	20.8	0.512897	0.000008	0.1442	0.512765	5.99
	11 DC-41	basalt	23.1	181	0.705409	0.000004	0.3692	0.704674	6.99	29.7	0.512861	0.000005	0.1418	0.512731	5.33
	11 DC-42	basalt	15.6	155	0.705058	0.000003	0.2911	0.704479	6.85	29.7	0.512854	0.000005	0.1389	0.512727	5.25
	11 DC-43	basalt	39.4	258	0.705618	0.000004	0.4418	0.704739	7.98	34.5	0.512851	0.000004	0.1393	0.512723	5.18
	11 DC-44	basalt	14.2	154	0.705062	0.000004	0.2667	0.704531	6.75	28.2	0.512866	0.000005	0.1442	0.512734	5.39

REFERENCES CITED

Wang, B.D., Wang, L.Q., Chung, S.L., Chen, J.L., Yin, F.G., Liu, H., Li, X.B., and Chen, L.X., 2016, Evolution of the Bangong-Nujiang Tethyan ocean: Insights from the geochronology and geochemistry of mafic rocks within ophiolites: Lithos, v. 245, p. 18–33, https://doi.org/10.1016/j.lithos.2015.07.016.